Utilization of an NNSS Receiver in the Explosion Seismic Experiments on the Prince Olav Coast, East Antarctica 2. Positioning

Kazuo SHIBUYA*, Kiyoshi ITO** and Katsutada KAMINUMA*

東南極，プリンスオラフ海岸で行われた爆破地震実験における航行衛星の利用 2. 位 置 決 定

渋谷和雄*・伊藤 潔**・神沼克伊*

要旨： 1波 (400 MHz) および2波 (150 MHz, 400 MHz) の NNSS 受信器による受信テストを昭和基地の天測点で行った．1波受信器による2次元的な (高さを固定した) 衛星測位は，多数の衛星軌道を用いて求められる平均位置から 200 m の標準偏差でばらつく．また，2波受信器による2次元的な (高さを固定した) 衛星測位は，多数の衛星軌道を用いて求められる平均位置から緯度方向に 25 m，経度方向に 50 m の標準偏差でばらつくことがわかった．上記の両者の平均位置は相対的に 70-80 m 以内である．いくつかの衛星軌道のドップラーデータを加算し3次元的な衛星測位が求められるが，軌道数に対する収束の見積もりを求めた．軌道数が3から7, 15, 25 とふえていくと衛星測位の平面的な誤差は 60 m, 40 m, 20 m, 10 m と減っていき，アンテナ高の誤差も 20 m, 10 m, 10 m, 5 m のように減っていく．解析の結果によると，天測測位と WGS-72 標準楕円体上の衛星測位には約 370-400 m のずれが見られ，またアンテナ高度と海抜高度にも 30±2 m の差がある．第21次南極地域観測隊による爆破地震実験では，27点の地震観測点の3次元的な衛星測位を15日間で行い，各点についてそれぞれ3から25の衛星軌道を受信して，実験の許容誤差以内で全点の位置決めを行うことができた．また，これらの観測点においてもアンテナ高度と海抜高度に 20-40 m の差が残った．上記高度差は近似的にジオイド高を与えるが，求められた値は，SEASAT 衛星の電波高度計解析から求められたジオイド図が示すこの地域の隣接海域の値と矛盾しない．10 m 以上の精度で衛星測位を行うためには，より多くの予報軌道を重ね合わせたり確定軌道を用いてもっと詳しい解析を行う必要がある．

Abstract: Performance tests of a one-wave (400 MHz) NNSS receiver and a two-wave (150 MHz and 400 MHz) NNSS receiver were made at Syowa Station, East Antarctica. The two-dimensional positioning by a one-wave receiver scattered with the standard deviation of about 200 m from the mean position determined by many passes. The two-dimensional positioning by the two-wave receiver scattered with the standard deviation of 25 m for the latitudinal direction and 50 m for the longitudinal direction, respectively. The mean position by many passes by the one-wave receiver and that by the two-wave receiver were relatively located within 70-80 m. Three-dimensional positioning was made by

* 国立極地研究所．National Institute of Polar Research, 9-10, Kaga 1-chome, Itabashi-ku, Tokyo 173.

** 京都大学理学部地震予知地域観測センター．Regional Observation Center for Earthquake Prediction, Faculty of Science, Kyoto University, Nasahara 944, Takatsuki-shi, Osaka 569.

accumulating doppler data of several passes and the estimate of convergence was made by taking the number of satellite passes as a parameter. Probable error in two-dimensional co-ordinates was shown to reduce from 60 m to 40 m, 20 m and further to 10 m according as the pass number was increased from 3 to 7, 15 and further to 25. The corresponding height error reduced from 20 m to 10 m and further to 5 m according as the pass number was increased from 3 to 7–15 and further to 25. There is a difference of about 370–400 m between the positioning by the satellite fixing on the WGS-72 earth ellipsoid and that by an astronomical observation. There is also the difference of 30±2 m between the antenna height and the elevation from the mean sea level at the same point. In the explosion seismic experiments by the 21st Japanese Antartic Research Expedition, three-dimensional positioning of most of the seismic stations was made within 15 days by receiving 3–25 passes at each station. There remained the difference of 20–40 m between the antenna height and the elevation for most of the seismic stations. The difference between the antenna height and the elevation gives the approximate geoid height, and the obtained values in this region of Prince Olav Coast are consistent with the geoid map obtained by the SEASAT altimetry data. In order to obtain the convergent procedures better than 10 m accuracy of the three-dimensional positioning, it is necessary to make more detailed analyses by using a number of broadcasted and/or precise ephemerides.

1. Introduction

In the explosion seismic experiments on the snow field, accurate and speedy positioning of sensor locations was important (ITO *et al.*, 1980). Since the positioning by the astronomical observations requires time and depends on good weather conditions, it was not appropriate from the operational point of view. The Navy Navigation Satellite System (NNSS) is an all-weather and world-wide positioning system whose utility in the low and intermediate latitudes is already ascertained. Table 1 shows an example of the rise-to-set time table of the NNSS satellites at Syowa Station (69°00′S, 39°35′E), SYO, in East Antarctica and Tokyo (35°45′N, 139°42′E), TYO, in Japan on April 27, 1980. Waiting time of the NNSS satellite (hereafter referred to only as the satellite) is comparatively shorter at SYO than at TYO. Since there are less electrical and mechanical obstacles in the receiving conditions of transmitted waves from the satellite in the antarctic region, an NNSS receiver may give us rather precise positioning without significant work time nor the user's skill.

The 21st Japanese Antarctic Research Expedition (JARE-21) prepared one altered 400 MHz NNSS receiver (hereafter referred to as the one-wave receiver) which was used mainly for recovering UTC (SHIBUYA and KAMINUMA, 1982, hereafter referred to as the first report), and one 150 MHz and 400 MHz receiver, JMR-1, which will hereafter be referred to as the two-wave receiver (JMR INSTRUMENTS INC., 1977). By receiving the above coherent-related two waves, refraction correction of the transmitted path in the ionosphere can be made (GUIER, 1961), which will enable us to obtain more precise positioning than that by the one-wave receiver. As described in the first report, the satellite transmits 157 words

Table 1. Alert table of NNSS satellites at Syowa Station and Tokyo on April 27, 1980. Time in UTC, elevation angle denotes height angle at the closest approach, while the direction indicates that the satellite rises from the given quadrant. Those which have the elevation angle between 15° and 75° are listed.

Syowa Station (69°00′S, 39°35′E)					Tokyo (35°45′N, 139°42′E)				
Rise	Set	Elevation angle	Satellite number	Direction	Rise	Set	Elevation angle	Satellite number	Direction
0100	0119	50	30130	03	0025	0043	19	30110	02
0139	0157	25	30200	01	0028	0044	17	30140	01
0245	0303	23	30110	01	0213	0233	64	30140	02
0246	0305	22	30130	03	0352	0410	23	30130	01
0306	0325	33	30190	03	0537	0557	48	30130	02
0322	0342	61	30200	01	0557	0617	63	30190	01
0429	0449	52	30110	01	0745	0801	18	30190	02
0436	0452	16	30140	01	1034	1053	56	30110	04
0452	0508	17	30190	03	1221	1240	20	30110	03
0508	0527	59	30200	02	1224	1240	16	30140	04
0616	0636	71	30110	02	1408	1428	67	30140	03
0620	0639	31	30140	01	1549	1607	23	30130	04
0655	0714	24	30200	02	1734	1754	49	30130	03
0800	0816	18	30130	01	1754	1813	61	30190	04
0805	0824	29	30110	02	1942	2000	18	30190	03
0805	0825	74	30140	01	2027	2046	26	30200	01
0944	1003	35	30130	01	2148	2207	23	30110	01
0952	1012	49	30140	02	2212	2232	38	30200	02
1005	1023	23	30190	01	2334	2354	48	30110	02
1141	1200	21	30140	02					
1149	1209	54	30190	01					
1221	1237	16	30200	04					
1317	1337	42	30130	02					
1335	1353	16	30110	04					
1336	1356	69	30190	02					
1407	1427	32	30200	04					
1507	1525	19	30130	02					
1523	1542	30	30110	04					
1525	1544	28	30190	02					
1710	1730	72	30110	04					
1710	1729	20	30140	04					
1739	1758	43	30200	03					
1857	1917	51	30110	03					
1858	1917	43	30140	04					
1924	1940	20	30200	03					
2036	2055	22	30130	04					
2044	2102	22	30110	03					
2055	2111	16	30190	04					
2224	2243	51	30130	04					
2231	2250	34	30140	03					
2243	2302	31	30190	04					

in every two minutes frame (Fig. 4 in the first report). The ephemerides to be broadcasted and stored in the memories on the satellite are regularly replaced and maintained by the U.S. Naval Astronautics Group. Since this report aims at discussing applicability of satellite positioning in the antarctic region, no detailed principles nor the scheme of the positioning method are mentioned here. It is to be mentioned only that both one-wave and two-wave receivers utilize the satellite with $15° < \theta < 75°$, where θ denotes the elevation angle at the closest approach, and that both receivers apply the short doppler method of a 24 or 30 seconds' doppler frame and apply also similar convergence conditions in the iteration procedures which are outlined in Fig. 5 of the first report.

2. Performance Experiments

The performance test of the one-wave receiver was made at point O in Fig. 6 during June 26–December 31, 1980. Figure 1 summarizes the scatters of the obtained two-dimensional positioning for the passes of each satellite identifier and the whole passes. The antenna height is fixed at 50 m above the WGS-72 earth ellipsoid by taking the approximate geoid height of 30 m at the point into consideration, which will be discussed later. Table 2 summarizes the mean latitude, the mean longitude and the standard deviations for both latitudinal and longitu-

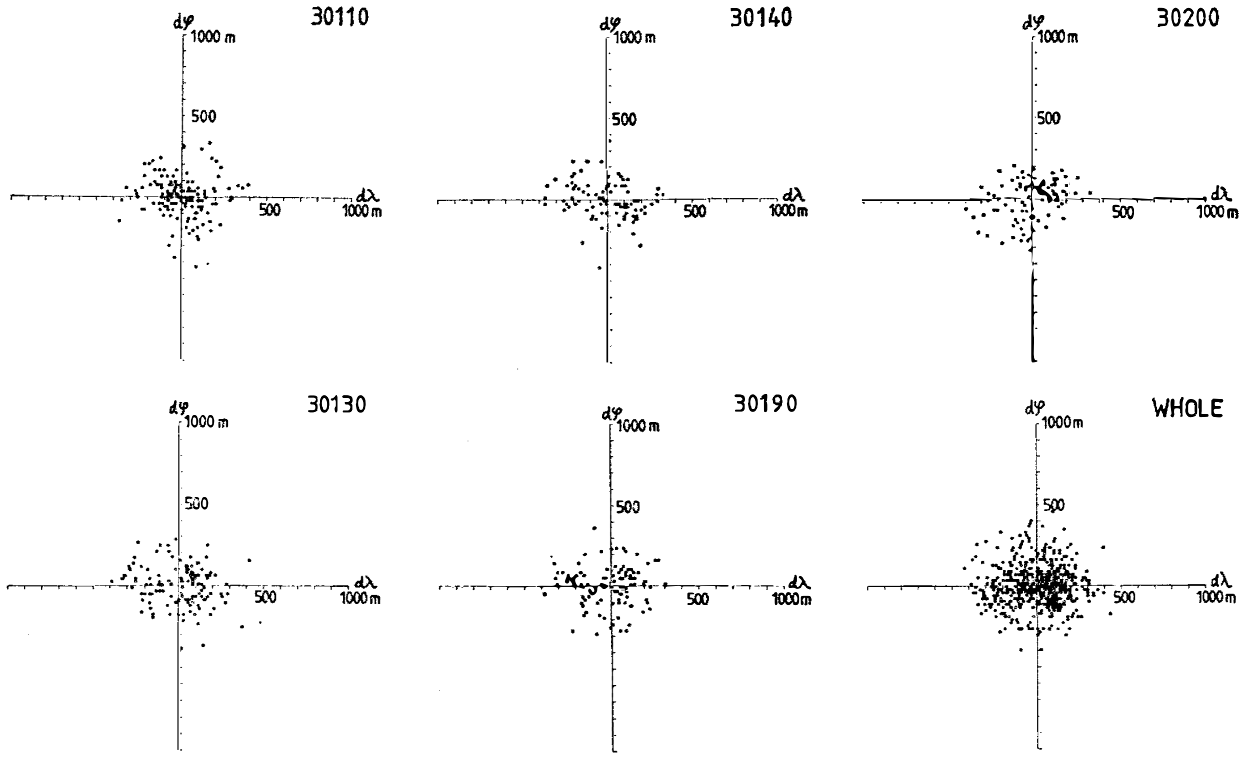

Fig. 1. Positioning of point O by using the one-wave receiver. dφ indicates difference from the mean latitude in the latitudinal direction which is positive for a northward direction. dλ indicates difference from the mean longitude in the longitudinal direction which is positive for an eastward direction. Numerals in the upper part of each figure indicate satellite identifier.

Table 2. Statistics of the two-dimensional satellite positioning by the one-wave receiver.

Satellite number	Number of passes	φ_m Mean latitude (S)	λ_m Mean longitude (E)	$\sigma_{d\varphi}$ Standard deviation of $d\varphi=\varphi-\varphi_m$	$\sigma_{d\lambda}$ Standard deviation of $d\lambda=\lambda-\lambda_m$	$\sqrt{\sigma_{d\varphi}^2+\sigma_{d\lambda}^2}$
30110	141	69°00′19.2″	39°34′46.2″	120 m	140 m	190 m
30130	130	69 00 17.4	39 34 47.4	120	160	200
30140	94	69 00 17.4	39 34 46.2	120	160	200
30190	106	69 00 17.4	39 34 45.6	120	150	200
30200	104	69 00 19.8	39 34 42.6	120	140	180
	575	69°00′18.3″	39°34′45.6″	120 m	150 m	200 m

Cf: antenna height above the WGS-72 ellipsoid is put as 50 m.

dinal directions. Though the scatters in Fig. 1 show sampled passes during the performance test, they will represent the characteristics of the positioning by the one-wave receiver in the antarctic region. The scatters in Fig. 1 have the standard deviation of 120–160 m without showing any particular azimuthal dependence (see also Table 2). The obtained mean position for the passes of each satellite identifier is located within the range of 60 m from that of other satellite identifier, which, however, is insignificant when the standard deviation of 120–160 m is taken into consideration. According to Fig. 1, the positioning by only one satellite pass may have a probable error of 200 m on the assumption that the mean position of a number of satellite fixings is convergent to a true position.

Figure 2 illustrates the results of a similar performance test of the two-wave

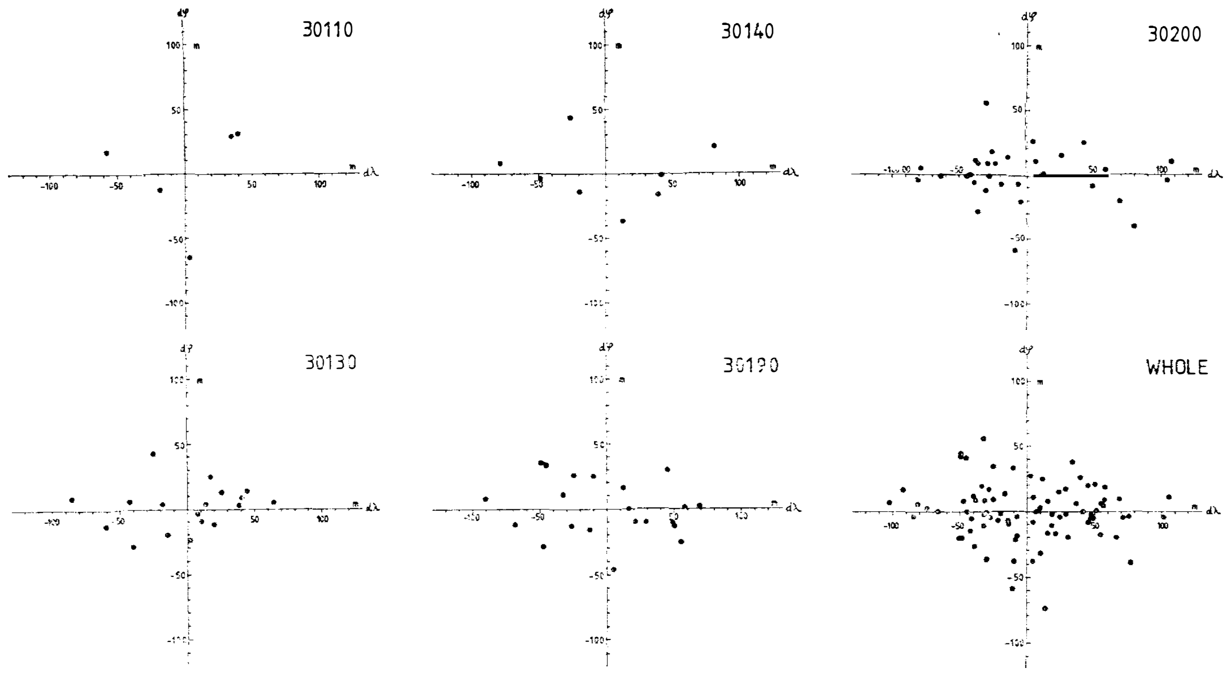

Fig. 2. Positioning of point A by using the two-wave receiver. Expressions of the co-ordinates are the same as those of Fig. 1.

Table 3. Statistics of the two-dimensional satellite positioning by the two-wave receiver.

Satellite number	Number of passes	φ_m Mean latitude (S)	λ_m Mean longitude (E)	$\sigma_{d\varphi}$ Standard deviation of $d\varphi=\varphi-\varphi_m$	$\sigma_{d\lambda}$ Standard deviation of $d\lambda=\lambda-\lambda_m$	$\sqrt{\sigma_{d\varphi}^2+\sigma_{d\lambda}^2}$
30110	5	69°00′19.96″	39°34′51.93″	36.1 m	36.3 m	51.2 m
30130	18	69 00 19.85	39 34 51.96	17.2	38.5	42.2
30140	8	69 00 19.69	39 34 49.10	23.4	49.6	54.8
30190	21	69 00 19.38	39 34 50.98	21.7	44.9	49.9
30200	33	69 00 19.63	39 34 50.84	21.0	47.4	51.8
	85	69°00′19.64″	39°34′51.01″	22.6 m	48.1 m	53.2 m

Cf: antenna height above the WGS-72 ellipsoid is put as 29 m.

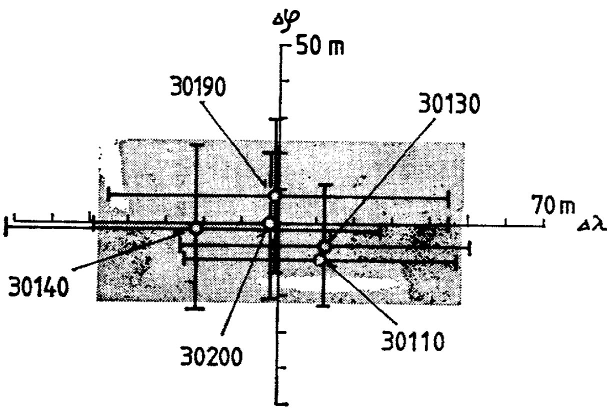

Fig. 3. Relative two-dimensional location of the mean position (open circle) and its standard deviations (cross) for each satellite identifier. Shaded box gives the probable error area of the mean position (origin of co-ordinates) which is determined by the whole passes.

receiver at point A in Fig. 6 during April 24–May 4, 1980. The antenna height is fixed at 29 m above the WGS-72 earth ellipsoid, the value is an approximate elevation of point A from the mean sea level. The scatters in Fig. 2 are in a range which is smaller by one order than that in the case of Fig. 1. It is also noticed that the obtained scatters have the range about twice as large in the longitudinal direction as that in the latitudinal direction. Table 3, which summarizes the mean latitude, the mean longitude and the standard deviations for the passes of each and whole satellite identifiers, is to be compared with Table 2. The reduction of the range of the scatters by introducing ionospheric refraction correction amounts to about 150 m. Figure 3 illustrates relative locations of the mean positions and their standard deviations for the passes of each satellite identifier. The mean position by the whole passes is taken as the center of co-ordinates. The results for 30110 and 30140 may have some uncertainty because the number of passes is comparatively small. As listed in Table 1, there often occurs that two satellites are going to rise simultaneously within a few minutes, and that a certain satellite identifier rises always behind. The small number of passes of 30110 and 30140 in Table 1 indicates that the tracking of the above two satellites was frequently masked by that of other satellite identifiers during the period of the performance test. Considering Fig. 3, there are no significant differences in the positioning results among different satellite identifiers. The location by only one pass may have the probable error of 20 m in the latitudinal direction and of 50 m in the longitudinal direction on the assumption that the mean position of a number of satellite fixings is convergent to the true position.

By accumulating doppler data of several passes which have good two-dimensional fixing, the most probable three-dimensional location can be estimated. The selected 100 passes including 85 passes in Table 3 were divided into four groups in accordance with the fixed sequential order. Each group has 25 passes and Table 4 illustrates the iterative change of such most probable locations of group I when the pass number, hereafter sometimes symbolized as n, is increased from 3 to 25. Let the end location of group I be the initial location of group II and the end location of group II be the initial location of group III and so on, similar changes to Table 4 can be obtained for each group of II–IV. Figure 4a shows the schematic illustration of the convergent procedure when the pass number is taken as a parameter. By taking the end position of each group as the center of coordinates, the differences of the iterative location in latitudinal ($\delta\varphi$) and longitudinal ($\delta\lambda$) planes at each iterative pass number are calculated and the results of the representative four cases ($n=3$, 7, 15 and 24) are illustrated. The circle shows the most probable location and the box gives the region of its probable error. Thinly shaded, thickly shaded, vertically lined and horizontally lined boxes indicate the regions of probable error in the cases of $n=3$, $n=7$, $n=15$ and $n=24$,

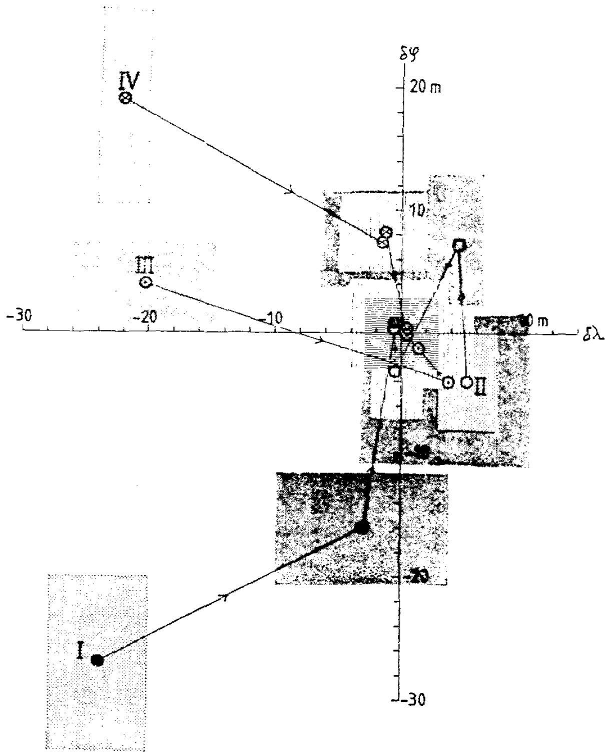

Fig. 4a. Schematic illustration of the changes of positioning as a parameter of pass number. For details, see the text.

Table 4. The iterative change of the most probable three-dimensional location of point A as a parameter of pass number. This table gives an example for group I.

Pass number	Latitude (S) φ	Longitude (E) λ	Antenna height	Probable error			Fixed time	Satellite identifier
				ε_φ	ε_λ	ε_h		
Initial	69°00′22.000″	39°35′24.000″	29.00 m					
1	69 00 21.013	39 34 48.965	29.00				116d07h28m	30200
2	69 00 20.548	39 34 49.722	43.00				116 09 38	30130
3	69 00 20.147	39 34 49.034	48.50	6.9	4.2	3.6	116 09 56	30140
4	69 00 19.810	39 34 51.198	74.62	5.2	11.1	10.8	116 12 54	30200
5	69 00 19.717	39 34 50.381	66.41	6.3	9.6	7.7	116 14 40	30200
6	69 00 19.802	39 34 50.534	60.14	5.2	7.6	3.9	116 17 12	30140
7	69 00 19.786	39 34 50.797	56.86	4.7	6.7	3.3	116 18 10	30200
8	69 00 19.589	39 34 51.069	59.71	5.0	6.1	2.8	116 18 58	30140
9	69 00 19.404	39 34 50.837	64.81	4.9	5.7	3.0	116 19 56	30200
10	69 00 19.304	39 34 50.996	67.71	4.5	5.4	2.8	116 20 30	30130
11	69 00 19.268	39 34 51.028	68.07	4.1	4.9	2.4	116 22 18	30130
12	69 00 19.269	39 34 51.042	66.54	3.8	4.4	1.9	116 22 36	30190
13	69 00 19.256	39 34 50.986	65.79	3.5	4.1	1.7	117 01 04	30200
14	69 00 19.178	39 34 50.906	66.72	3.5	3.8	1.4	117 02 12	30190
15	69 00 19.235	39 34 51.034	67.88	3.6	3.7	1.3	117 02 46	30200
16	69 00 19.171	39 34 51.081	68.44	3.5	3.5	1.2	117 03 34	30110
17	69 00 19.167	39 34 51.088	68.39	3.3	3.3	1.2	117 03 58	30190
18	69 00 19.188	39 34 51.322	68.08	3.1	2.8	1.1	117 06 18	30200
19	69 00 19.229	39 34 51.373	66.96	3.0	2.7	1.0	117 08 58	30110
20	69 00 19.235	39 34 51.305	66.07	2.9	2.7	0.9	117 10 34	30130
21	69 00 19.260	39 34 50.996	64.28	2.9	2.9	0.9	117 13 34	30200
22	69 00 19.217	39 34 51.073	63.24	3.0	2.8	0.9	117 14 10	30130
23	69 00 19.220	39 34 50.999	64.06	2.9	2.7	0.8	117 17 04	30200
24	69 00 19.260	39 34 51.073	62.85	2.8	2.7	0.8	117 18 48	30200
25	69 00 19.263	39 34 51.063	62.65	2.7	2.6	0.7	117 21 28	30130

respectively. As for group I, the position at $n=3$ is located at solid circle I ($\delta\varphi=-27.3$ m, $\delta\lambda=-23.9$ m) with the uncertainty of ± 6.9 m for latitudinal and ± 4.2 m for longitudinal directions against the end location. When the pass number is increased to 7, the iterative most probable location shifts to the solid circle at ($\delta\varphi=-16.2$ m, $\delta\lambda=-3.1$ m) with the corresponding probable error area of ± 4.7 m for latitudinal and ± 6.7 m for longitudinal directions, though the pass line from the point at $n=3$ to that at $n=7$ is not so straight as indicated by the arrowed solid line in Fig. 4a. Likewise, the most probable location shifts to the solid circle in the vertically lined box and further to that in the horizontally lined box when the pass number is increased to 15 and further to 24. Iterative location of any group comes nearer to the corresponding end location mostly from the westward direction except group II and the probable error region becomes smaller according as the pass number is increased. The effect of increment in pass number, however, is slow after $n=15$ where the offset from the end location $\delta r=\sqrt{\delta\varphi^2+\delta\lambda^2}$ is around 4–10 m. It is noted that the end location of one group is somewhat different from that of another group as summarized in Table 5. There exist some offsets among the centers of co-ordinates of $\delta\varphi-\delta\lambda$ planes for groups I–IV. Such offsets are neglected and the obtained four planes are superposed on Fig. 4a of the common center of co-ordinates. Figure 4b illustrates

Table 5. End location of each group after three-dimensional positioning is made by using 25 passes.

Group	Latitude (S)	Longitude (E)	Antenna height
I	69°00′19.263″	39°34′51.063″	62.65 m
II	69 00 19.214	39 34 51.220	60.96
III	69 00 19.001	39 34 51.077	58.04
IV	69 00 18.930	39 34 50.834	62.32

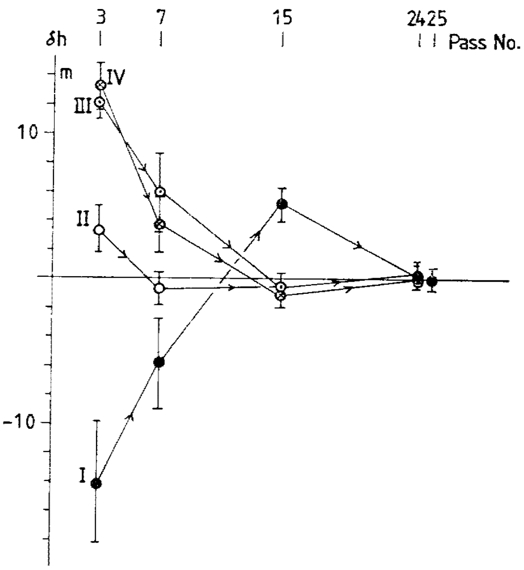

Fig. 4b. The change of the antenna height as a parameter of pass number. For details, see the text.

the iterative change of the antenna height which corresponds to the two-dimensional results in Fig. 4a. The circle indicates the most probable height, while bars indicate probable errors at the pass number given in the upper part of Fig. 4b. The difference between the iterative antenna height and the end antenna height is around 10–20 m at $n=3$, which becomes small around 5–10 m when the pass number is increased to 7, and also becomes gradually small toward 1–2 m with smaller probable errors according as the pass number approaches 25, though the path of convergence is not so straight as indicated by the arrowed solid line in Fig. 4b.

When the pass number is fixed, relative locations of the iterative positions of groups II–IV against those of group I for the representative cases of $n=3$, $n=7$, $n=15$ and $n=25$ are illustrated in Fig. 5a. For example, the iterative location at $n=3$ of group II has the offset of $\Delta\varphi=24.9$ m for the latitudinal direction and of $\Delta\lambda=31.1$ m for the longitudinal direction against the iterative location at $n=3$ of group I. The above offset position is marked by solid circle II3 in Fig. 5a. Similarly, the offset position of group III and group IV against that of group I at $n=3$ are plotted by marks III3 ($\Delta\varphi=38.9$ m, $\Delta\lambda=3.7$ m) and IV3 ($\Delta\varphi=56.3$ m, $\Delta\lambda=0.6$ m), respectively. The group of marks II7–IV7, II15–IV15 and II25–IV25 can also be obtained and plotted in the corresponding $\Delta\varphi-\Delta\lambda$ plane, respectively. Since reference locations of group I shift according as n is increased, the center of co-ordinates in one plane is somewhat offset to that of another plane. Such offsets are neglected and the obtained four $\Delta\varphi-\Delta\lambda$ planes are superposed on the same Fig. 5a of the common center of co-ordinates. Figure 5b illustrates the

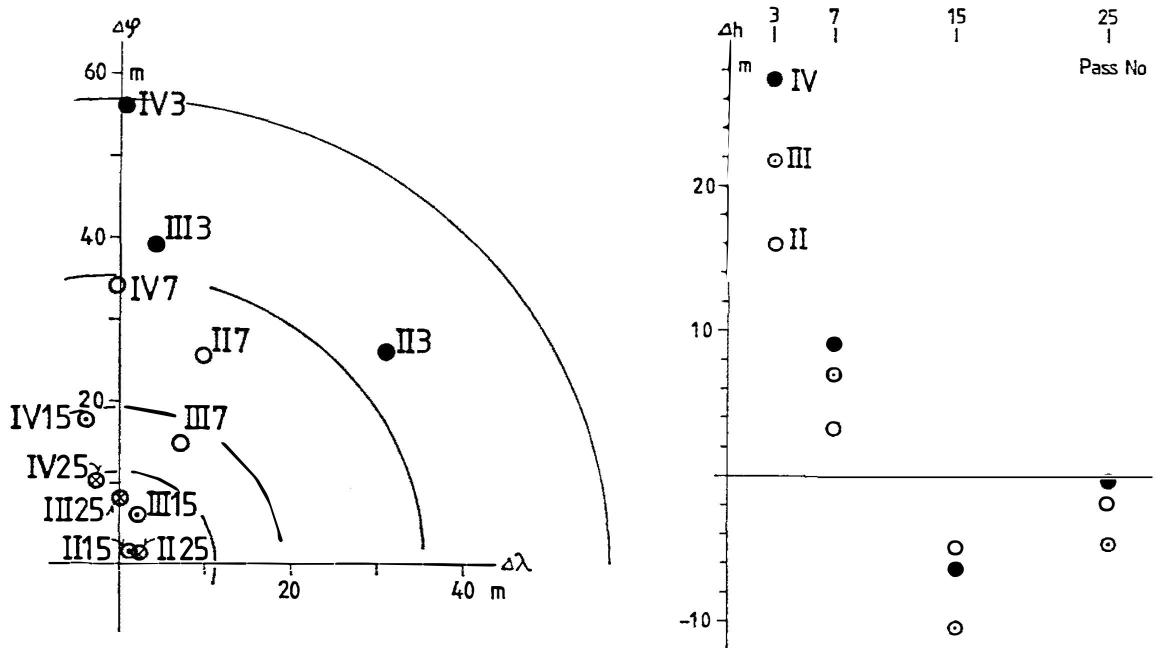

(a) (b)

Fig. 5. (a) Relative location of the iterative position of groups II–IV against the corresponding iterative position of group I with the fixed pass number. For details, see the text.
(b) The difference of the iterative antenna height of groups II–IV against that of group I with the fixed pass number.

difference of the antenna height at the iterative pass number of groups II–IV from that at the corresponding pass number of group I. Open circles indicate the results of group II, while dotted and solid circles indicate those of groups III and IV, respectively. The results correspond to the two-dimensional results in Fig. 5a.

An example of the iterative change of the three-dimensional positioning by taking the fixing sequence or the pass number as a parameter was given in Figs. 4 and 5. The accuracy of the satellite positioning must be estimated by taking the changes in both $\delta\varphi-\delta\lambda$ plane and $\Delta\varphi-\Delta\lambda$ plane into consideration. The positioning results may be slightly different if the setting of the initial position at each group and/or the selection of passes and their combinations are altered. However, the change of the results seems to be insignificant to alter the above obtained rough estimate of the convergence as a parameter of pass number.

3. Results and Discussions

A performance test for estimating the applicability of NNSS positioning in the antarctic region was made by using a one-wave receiver and a two-wave receiver and by receiving multi-passes of the NNSS satellite doppler data at the fixed points. The obtained results may be summarized as follows: (a) The two-dimensional positionings by a one-wave receiver scatter with the standard deviation of about 200 m from the mean position. There are no significant differences in the positioning results among different satellite identifiers. The mean position of the whole passes is located within the range of 70–80 m from the mean position given by the several passes received by the two-wave receiver (Table 2 or 3). (b) The two-dimensional positionings by the two-wave receiver scatter with the standard deviation of 25 m for the latitudinal direction and 50 m for the longitudinal direction, respectively. There are no significant differences in the positioning results among different satellite identifiers. (c) Three-dimensional positioning can be made by accumulating doppler data of multi-passes. The estimate of the convergence as a parameter of pass number may be given in Table 6.

Since the antenna height is fixed at the elevation from the mean sea level in the case of (b), it is probable that the error of 30 m (see Table 5) in the antenna height over the WGS-72 reference ellipsoid may affect the positioning errors.

Table 6. The estimate of convergence in the three-dimensional positioning as a parameter of pass number. σ_r is given by the larger value between $\delta r=\sqrt{\delta\varphi^2+\delta\lambda^2}$ and $\Delta r=\sqrt{\Delta\varphi^2+\Delta\lambda^2}$. σ_h is given by the larger value between δh and Δh, where the above notations are given in the expressions in Figs. 4 and 5.

Pass number	σ_r	σ_h
3	60 m	20 m
7	40	10
15	20	10
25	10	5

When the two-dimensional positionings are re-calculated for several passes with large discrepancies by only altering the antenna height of 29 m to a fixed value of 60 m, the discrepancies from the mean position reduce to 30 m without showing significant azimuthal dependence. It is thus suggested that the error in the antenna height results in the positioning error of the same value rather in the longitudinal direction than that in the latitudinal direction and that the error adds to the probable radial error of 25–30 m.

Figure 6 summarizes the satellite positioning of points A and O on the map. Point O is positioned by the one-wave receiver at O_1 on the map and reduced to point A_1 by subtracting $\overrightarrow{OA}$ from $\overrightarrow{AO_1}$. The open circle gives the probable error area of 200 m radius (Table 2) in the positioning. Point A_2 indicates the most probable two-dimensional positioning of point A which is obtained by using the two-wave receiver. The shaded box gives the probable error area which is characterized by the standard deviations listed in Table 3. Point A_3 shows a most probable location of point A on the map which is obtained by the three-dimensional satellite positioning and by using 25 passes recorded by the two-wave receiver, where the probable error area is marked by the solid circle. As shown in Fig. 6, the satellite positioning A_3 of point A on the standard earth ellipsoid WGS-72 (a=6378135 m, f=1/298.26) has a shift of about 370–400 m toward a

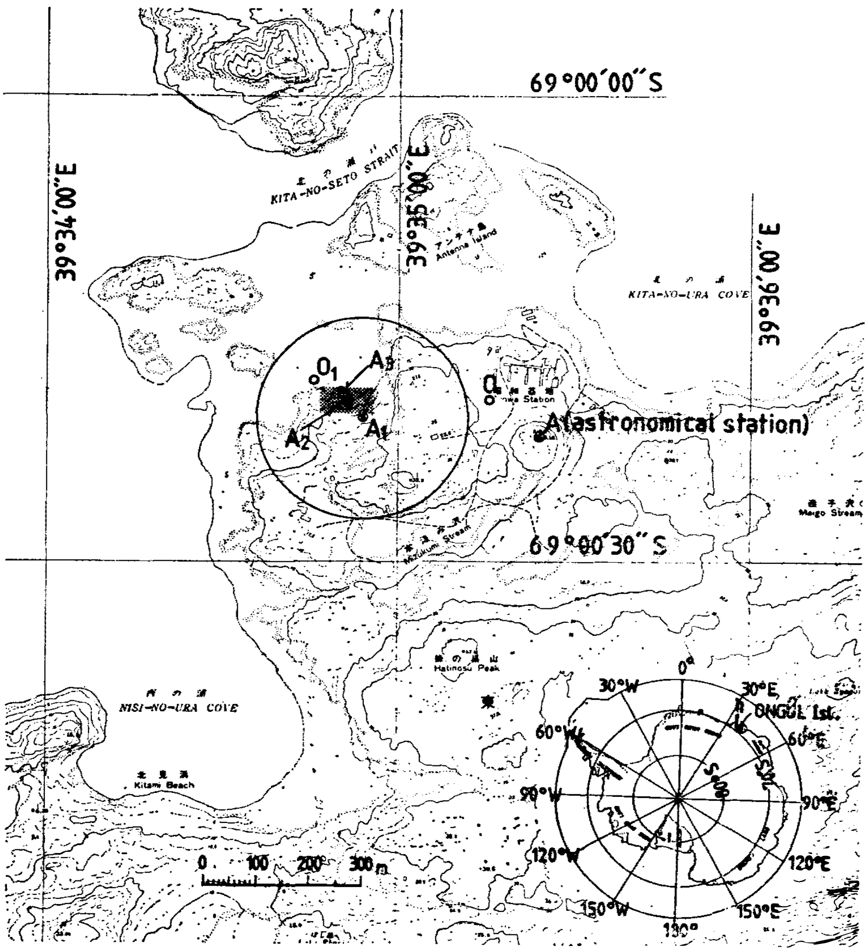

Fig. 6. Summary of the satellite positioning of point A. For details, see the text.

west-northwest direction with respect to point A.

Point A is the astronomical station at Syowa Station, and the reference ellipsoid International Geodetic System 1967 (a=6378140 m, f=1/298.257) for determining geodetic latitudes and longitudes in the surrounding area was established by setting $\xi=\eta=0$ at point A, where ξ and η are northward-component and eastward-component of the deflection of the plumbline, respectively. However, the difference of the antenna height (60±2 m) and the elevation from the mean sea level (29.18 m) gives the approximate geoid height of 30±2 m at the astronomical station A. The inconsistence of point A_3 against point A can be considered to come from the overall effect of the errors in the satellite positioning, inaccuracies of the astronomical positioning of ±4″ in the latitudinal direction and ±12″ in the longitudinal direction (GEOGRAPHICAL SURVEY INSTITUTE, 1981) and the deflection of the plumbline at the astronomical station.

In the explosion seismic experiments by JARE-21, 27 seismic detectors were located along the traverse S-H-Z route from S16 (Mikaeri Terrace) to the Japanese inland station Mizuho as shown in Fig. 7. Each sensor was closely positioned to the traverse survey station which was made by JARE-14 (NARUSE and YOKOYAMA, 1975). Sensor locations could be made mostly by the three-dimensional satellite positioning during October 20–November 4, within the acceptance error for explosion seismic experiments. Table 7 summarizes the elevation from the mean sea level (NARUSE and YOKOYAMA, 1975) and the antenna height at the same station. Time interval from the traverse survey by JARE-14 to the explosion seismic experiments by JARE-21 amounts to 7–8 years. When the height change by snow accumulation (ablation) and/or by flow of icesheet in that interval does not exceed 10 m, there remains the difference between the above two heights of 20–40 m geoid heights for most of the stations. Figure 8 shows an example of the geoid map in the antarctic region which is obtained by the SEASAT altim-

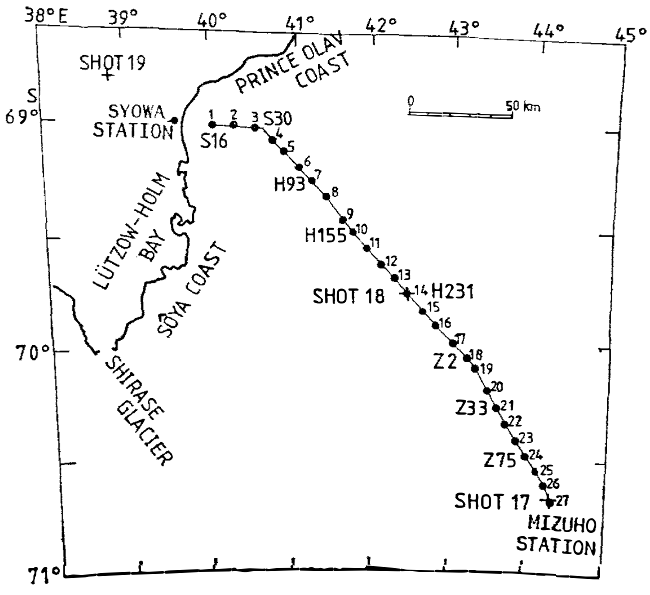

Fig. 7. Sensor locations in the explosion seismic experiments by JARE-21 along S-H-Z route.

Table 7. Summary of the elevation and the antenna height at the sensor locations (traverse stations) along the S-H-Z route. T indicates the traverse survey point by JARE-14 (NARUSE and YOKOYAMA, 1975). Elevation at the station without T is an interpolated value. Star indicates that the satellite fixing was made in a loose mode. Error in antenna height is a calculated standard deviation by the two-wave receiver.

No.	Station	h_1 Elevation from mean sea level	h_2 Antenna height	$\Delta h=h_2-h_1$ Geoid height	Pass number
1	S16-1	562 m	594± 2 m	32 m	10
2	S22	757	777± 2	20	4
3	S27-3	926	951± 8	25	3
4	H17	T1035	1062± 2	27	8
5	H48-1	T1133	—	—	2
6	H74-1	T1207	—	—	2
7	H93	T1270	1307± 4	37	10
8	H113-1	T1339	1394±11	55	*9
9	H137	T1396	1425± 4	29	3
10	H155	T1465	1499± 2	34	3
11	H174	T1524	1493±20	−31	3
12	H194	T1560	1559±14	− 1	3
13	H213	T1617	1658±17	41	*5
14	H231	T1667	1693± 3	26	12
15	H253	T1739	1773± 3	34	10
16	H272	T1789	1831± 6	42	*6
17	H295	1881	1905± 1	24	25
18	Z2	T1926	1957± 1	31	10
19	Z11-1	T1984	1960±27	−24	*4
20	Z22-1	T2011	2040± 6	29	3
21	Z33	T2064	2099± 1	35	7
22	Z42-1	T2097	2142±10	45	3
23	Z60-1	T2118	2139± 2	21	23
24	Z75	T2159	2189± 4	30	7
25	Z85	T2161	2195± 7	34	3
26	Z94	T2186	2228± 5	42	4
27	Mizuho Station	2230	2259± 1	29	17

etry data (SEGAWA, 1982). The obtained value of 20–40 m by the NNSS positioning on the Prince Olav Coast is consistent with the map in Fig. 8, though the uncertainties due to the use of different standard earth ellipsoid between WGS-72 for NNSS satellites and GEM10B (a=6378138 m, f=1/298.257) for SEASAT have to be taken into consideration.

It was shown that the three-dimensional satellite positioning can be improved by increasing the pass number. However, so long as the analyzed four sets with a total of 100 passes are concerned, the most probable position did not exhibit random scatters within a circle of a certain radius but shifted slightly toward

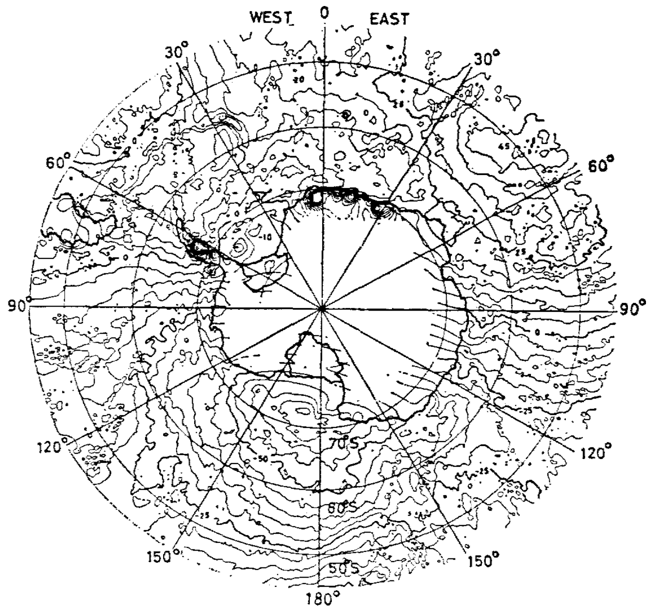

Fig. 8. Geoid map in the antarctic region, redrawn from SEGAWA *(1982).*

north, the more the end point which was obtained by using 25 passes was reset to the initial point for the succeeding doppler data of 25 passes (Table 5). The accuracy of the NNSS positioning by the broadcasted ephemerides depends on the errors in the broadcasted orbital data and may be affected by the occasional change of the ephemerides. Therefore, it may be necessary to make a detailed analysis by using the precise ephemerides and receiving more satellite passes in order to obtain more precisely convergent satellite positioning in the antarctic region.

Acknowlegments

The authors express their sincere thanks to Dr. S. KAWAGUCHI and all the members of JARE-21 for their encouragement and assistance in the experiments on the snow field. This research was partly financed by the budget for JARE, entitled to the "Geophysical investigations of the crust and upper-mantle structure of the Prince Olav Coast, East Antarctica (representative: T. NAGATA)".

References

GEOGRAPHICAL SURVEY INSTITUTE, comp. (1981): Catalog of JARE Geodetic Survey Data. Tokyo, National Institute of Polar Research, 125 p.

GUIER, W. H. (1961): Ionospheric contributions to the doppler shift at VHF from near-earth satellites. Proc. IRE, **49**, 1680–1681.

ITO, K., IKAMI, A., SHIRAISHI, K., SHIBUYA, K., KAMINUMA, K. and KATAOKA, S. (1981): Jinkô jishin ni yoru Nankyoku tairiku no chikaku kôzô (2)—Dai-21-ji Nankyoku Kansokutai ni yoru jikken—(Crustal structure of East Antarctica as revealed by explosion seismology (2)—Experiments by the 21st Japanese Antarctic Research Expedition). Jishin Gakkai Kôen Yokôshû Showa-56-Nendo Shûki Taikai (Programme and Abstracts, the Seismological Society of Japan, 1981(2)), Kyoto, Jishin Gakkai, 36.

JMR INSTRUMENTS INC. (1977): The JMR-1 Doppler Survey Set, Description and Application. Chatsworth, Cal., 24 p (Document No. JMR 73288-3).

NARUSE, R. and YOKOYAMA, K. (1975): Position, elevation and ice thickness of stations. JARE Data Rep., **28** (Glaciol.), 7–47.

SEGAWA, J. (1982): Evaluation of the geoid based on the SEASAT altimetry data at sea around Antarctica. Nankyoku Shiryô (Antarct. Rec.), **76**, 55–62.

SHIBUYA, K. and KAMINUMA, K. (1982): Utilization of an NNSS receiver in the explosion seismic experiments on the Prince Olav Coast, East Antarctica 1. Recovered UTC. Nankyoku Shiryô (Antarct. Rec.), **76**, 63–72.

(*Received February 25, 1982; Revised manuscript received April 19, 1982*)